

# Extended Node Method for Steady-State Heating Network Calculation based on Electric Analogies

Daniela Vorwerk  
Electrical Power Systems  
Helmut Schmidt University /  
University of the Bundeswehr  
Hamburg, Germany  
daniela.vorwerk@hsu-hh.de

Detlef Schulz  
Electrical Power Systems  
Helmut Schmidt University /  
University of the Bundeswehr  
Hamburg, Germany  
detlef.schulz@hsu-hh.de

**Abstract**— In the context of a multi-energy-grid, the consideration of various energy carriers on the same level is beneficial. This work shows the development of heating network components in electric analogies for their definition and usage in the node-based Extended Node Method. The method enables an efficient iteration algorithm for finding of stable steady-state operation points, even for extended network topologies. Three different thermal equivalent circuit diagrams, a ladder-, Pi- and T-model, describing the thermal behavior of heating pipelines are presented. They simultaneously fulfill the thermodynamic energy balance as well as the electrical equivalent circuit diagram correlations. The influence of the spatial resolution is tested using a single-line model. Moreover, a steady state calculation is also performed for an 18-node sample network. All results are compared with Simulink/Simscape and show satisfactory agreements.

**Keywords**—electric circuit diagrams, district heating grid, sector-coupling, grid calculation method

## I. INTRODUCTION

Joint planning of heat supply via the energy networks electricity, gas and district heating offers synergies and advantages on the path to the decarbonization of the heating sector. In densely settled regions district heating networks (HN) represent an alternative to fossil fuels such as oil or natural gas [1] and can be used from industrial waste heat recovery [2]. For planning purposes and cooperation of such a multi-energy-grid, consisting of different energy carriers, a joint consideration on a common level is beneficial. In this field, this work makes its contribution: The components of a HN are modeled using electrical analogies to describe the governing hydraulic and thermal effects for the steady-state. Clear aspects of novelty are the parameters of the electrical equivalent circuit diagrams (EC) presented here and their embedding in the “Extended Node Method” (ENM) from [3, 4]. For this purpose, conductance matrices for the components are derived and the definition of the nodes and the setup of the system of equations (SOE) are presented. On that basis, a complete equivalent electrical network (EEN) is derived to find hydraulically and thermally stable steady states also for extensive HN based only on node equations. With the help of this method, a simple link between HN and electric systems is enabled and considering them together supports designing sustainable energy concepts with respect to more than one energy carrier [5, 6]. Electric analogies are already used for hydraulic considerations in gas networks e.g. in [7, 8]. For electrical analogies in HN or the simultaneous consideration with electric power networks, the following references are to be named: In [9] enthalpy transport through

a heating pipe (HP) including losses to the environment is described using EC. A separation between hydraulic and thermal system adopted here is applied. An essential difference is the formulation of the EC for the temperature drop between individual control volumes (CV). Height differences and the impact of the pressure in the enthalpy are neglected for the thermal system. In [10] an approach for a dynamic EC for a Combined Heat and Power plant is proposed. Electrical components are applied to describe the thermal system, but a different flow quantity is proposed and steady-state operation of extended HN is not a topic in [10]. In [11], the interaction of electrical and thermal systems is addressed with time scale characteristics based on a multi-energy flow model. The modeling of the HP is done by conventional descriptions for the head loss and nodal equations, there is no development of conductances. In [12] a novel power flow algorithm for steady-state combined electric and heat considerations is presented. The thermal consideration is embedded in the AC *Newton-Raphson* algorithm. But the laws of fluid mechanics do not explicitly follow the representation by EC. In [13] also EC are used for a HP but the focus is particularly on the dynamic behavior of individual HP. It is not clear how the method in [13] contributes to finding operation points in HN. The paper is structured as follows: The basic fundamentals and the hydraulic and thermal EC development of HP as well as heat sources and consumers are taken up in Section II. In Section III, the definition of grid nodes and the building of the SOE in the ENM context are carried out and the thermal-hydraulic iteration algorithm is presented. Subsequently, sample study cases based on two different HN topologies and their results for steady-state operation are presented and compared with results from Simulink/Simscape in Section IV. A short conclusion and an outlook are given in Section V.

## II. HEATING NETWORK COMPONENTS FOR THE EXTENDED NODE METHOD

The chosen potential and flow variables for the hydraulic as well as the thermal system of a HN are listed in Table I. The equivalent of voltage in electrical systems is the pressure  $p$  in hydraulic systems and the flow variable as equivalent to the

TABLE I. OVERVIEW OF POTENTIAL AND FLOW QUANTITIES FOR A HEATING NETWORK AND THEIR ELECTRIC ANALOGIES.

Quantity	Electric	Hydraulic	Thermal
Potential	$u$ in V	$p$ in Pa	$T$ in K
Flow quantity	$i$ in A	$\dot{m}$ in kg/s	$\dot{H}, \dot{Q}$ in J/s

current  $i$  is the mass flow rate  $\dot{m}$ . For the thermal system the temperature  $T$  is set as the potential quantity. The quantity  $\dot{H} = \dot{m}c_p T$  as a reduced form of the enthalpy is set as the corresponding mass-bound flow variable, resp.  $\dot{Q}$  for the not mass-bound heat flow rates. The definition of  $\dot{H} = f(T)$  chosen here does not strictly speaking correspond to the thermodynamically exact definition of enthalpy, since it contains only the temperature component. But due to simplicity,  $\dot{H}$  is nevertheless referred to as enthalpy flow rate in the following work.

#### A. The Extended Node Method

In this work, the HN shall be embedded in the context of the ENM (see e.g. [3, 4]) to display it with its hydraulic and thermal properties as an EEN. The ENM originally serves for the efficient calculation of electric transients in expanded networks and was extended to isothermal gas networks in [14]. Because of its unique definitions of individual grid components and nodes the SOE can be built as an Algebraic-Differential-Equation-System (ADES). It is based only on node equations and hence the elaborate formulation of mesh equations in extensive networks is avoided [4]. The components are classified according to their terminal behavior regarding currents  $i$  and voltages  $u$ . There are three different types of components: L-components with inductive behavior, R-components with resistive behavior and C-components with capacitive behavior. Each component is also defined depending on their number of terminals as 'A' (one-terminal), 'AB' (two-terminal) or 'ABC' (three-terminal) component. The nodes' classification depends on the connected components. For the detailed method's documentation reference is made to [4].

#### B. Modeling of Heating Pipelines

For the conversion of a HP to its steady-state EC model, the governing laws of fluid mechanics are consulted:

$$\frac{\partial(\rho v)}{\partial x} = 0 \quad (1)$$

$$\frac{\partial p}{\partial x} + \frac{\lambda}{2D} \rho v |v| + \rho g \sin \alpha = 0 \quad (2)$$

$$-\frac{\partial}{\partial x} \left( \rho v \left( c_v T + \frac{p}{\rho} + \frac{v^2}{2} + gz \right) \right) + \rho \dot{q} = 0 \quad (3)$$

representing the conservation of mass (1), momentum (2) and energy (3) in the stationary form. Water as the here considered energy carrier is assumed as ideal liquid. Hence, it is regarded incompressible ( $\rho = \text{const.}$ ) and for the specific heat capacities it holds  $c_v = c_p$ . Due to the incompressibility, there is no velocity change in  $x$ -direction. Regarding the energy conservation, neglecting the pressure term due to low pressure drop  $\frac{\partial p}{\partial x} \approx 0$  is a common assumption [9, 15]. Here, two considerations are made: A simplified thermal system is built neglecting the pressure and height terms in the energy conservation (3), whereas also a complete model including pressure and potential energy is developed. In the course of this work it is clarified, how the type of consideration, simplified or complete, affects the development of the ECs. Axial heat conduction within the water as heat transfer medium shall be neglected here. For the derivation of

network models for HP, (1)-(3) are spatially discretized by defining segments of length  $dx = l$  with their terminals A located at  $x = 0$  and B at  $x = l$ . Each segment corresponds to a CV with its inner volume  $V = \pi D_i^2 l / 4 = Al$ , dependent on the HP's inner diameter  $D_i$ . The mass flow rates  $\dot{m}_A$  and  $\dot{m}_B$  as well as the enthalpy flows  $\dot{H}_A = \dot{m}_A c_p T_A$  and  $\dot{H}_B = \dot{m}_B c_p T_B$  of the heat carrier are defined as positive into each segment at the terminals. In the following approach, the modeling of the forward system of a HN is focused, while the return system is neglected.

##### 1) Hydraulic Pipeline model:

Using the beforementioned spatial discretization and the correlation  $\dot{m} = \rho v A$ , (2) can be rewritten and delivers the specific hydraulic SOE for a segment solved for the terminal mass flow rates to:

$$\begin{pmatrix} \dot{m}_A \\ \dot{m}_B \end{pmatrix} = \begin{pmatrix} \frac{2D_i A}{\lambda |v|} & -\frac{2D_i A}{\lambda |v|} \\ -\frac{2D_i A}{\lambda |v|} & \frac{2D_i A}{\lambda |v|} \end{pmatrix} \begin{pmatrix} p_A \\ p_B \end{pmatrix} + \begin{pmatrix} -\frac{\lambda D_i \rho g A \sin \alpha}{2 |v|} \\ \frac{\lambda D_i \rho g A \sin \alpha}{2 |v|} \end{pmatrix} \quad (4)$$

$$= \mathbf{G}_{h,RP} \mathbf{p}_R + \dot{\mathbf{m}}_{qR}$$

With the hydraulic conductance  $G_{h,R}$ , depending on the HP's geometric parameters, the flow velocity  $v$  and the friction factor  $\lambda$ . The vector  $\dot{\mathbf{m}}_{qR}$  includes the so-called source mass flows and only occurs with a height difference between the terminals A and B [14]. According to the ENM component definition in [4], (4) represents a two-terminal component with resistive behavior, hence it shall be called an R-AB component [14]. The specific EC is pictured in Fig. 1.

##### 2) Thermal Pipeline model

With the given sign convention for the enthalpy flow rates the steady-state energy conservation in (3) in a simplified and the complete form can be expressed by:

$$\text{Simplified: } \dot{H}_A - \dot{Q}_{\text{amb}} + \dot{H}_B = 0, \quad (5)$$

$$\text{Complete: } \dot{H}_A + |\dot{m}| c_p \Delta e - \dot{Q}_{\text{amb}} + \dot{H}_B = 0 \quad (6)$$

with  $\Delta e = \frac{p_A - p_B}{\rho c_p} + \frac{g(z_A - z_B)}{c_p}$  representing the rest of the potential in K and  $\dot{Q}_{\text{amb}}$  representing the heat flow rate across a CV's sheathing to the environment. In contrast to the enthalpy flows, this heat is not massbound. According to Fourier's law, it can be determined as

$$\dot{Q}_{\text{amb}} = G_{\text{th,CV}} (T_{\text{CV,abs}} - T_{\text{amb}}). \quad (7)$$

$T_{\text{CV,abs}}$  represents the CV's absolute temperature,  $T_{\text{amb}}$  the ambient temperature and  $G_{\text{th,CV}}$  is the thermal conductance depending on the HP's geometry as well as material properties (see [9]). Assuming a constant and known ambient

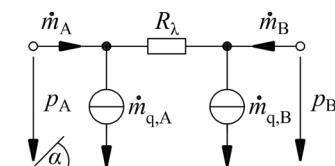


Fig. 1. Electric circuit for hydraulic modeling of a heating pipeline.

temperature  $T_{\text{amb}}$ , the following definitions are set for the regarded system:

$$T_A \equiv T_{A,\text{abs}} - T_{\text{amb}}, T_B \equiv T_{B,\text{abs}} - T_{\text{amb}}. \quad (8)$$

Thus, the system is defined with the excess temperature compared to the environment. This allows the parameterization of the ECs with respect to the defined zero potential  $T_0 = T_{\text{amb}}$ . In the following, three different EC, a ladder-(L-) in Fig. 2(a), a Pi- in Fig. 2(b) and a T-model in Fig. 2(c), for the thermal description of HPs resp. their CVs are presented. They are inspired by typical electric line modeling and represent a spatially lumped representation of the original distributed fluid mechanical system. The corresponding parameters like the branch resistance  $R_{\text{th,long}}$  and the conductance matrix  $\mathbf{G}_{\text{th,R}}$  are listed in Table II. These depend on the results of the mass flows from (4) and must therefore be redetermined for other flow conditions. The main difference between the three models is the formulation of the heat flow rate  $\dot{Q}_{\text{amb}}$  released to the environment. For the L-model it is assumed that the heat  $\dot{Q}_{\text{amb}}$  is completely dissipated at the temperature level  $T_A$  over the entire outer surface of a CV. Thus, it holds  $\dot{Q}_{\text{amb}} = G_{\text{th,cr}} T_A$ . In the case of the Pi- EC, on the other hand, heat is dissipated at the temperature level  $T_A$  over half of the outer shell surface and at the temperature level  $T_B$  over the other half, i.e.  $\dot{Q}_{\text{amb}} = G_{\text{th,cr}}/2 (T_A + T_B)$ . In the T-EC, a linearized mean temperature  $T_m = (T_A + T_B)/2$  is introduced for heat dissipation over the surface. The calculation of the dissipated heat  $\dot{Q}_{\text{amb}}$  is then done accordingly as for the Pi-model. In contrast to the solution of the actual partial differential equation (3), where the temperature course within a HP results as a decaying exponential function (see e.g. [15]), a linearized model is achieved using the discretized EC. The associated branch resistors  $R_{\text{th,long}}$  have been derived

fulfilling the simplified energy balance in (5) as well as the ECs' mesh equations. The components' SOE have the shape:

$$\text{Simplified: } \begin{pmatrix} \dot{H}_A \\ \dot{H}_B \end{pmatrix} = \mathbf{G}_{\text{th,R,AB}} \begin{pmatrix} T_A \\ T_B \end{pmatrix} \quad (9)$$

$$\text{Complete: } \begin{pmatrix} \dot{H}_A \\ \dot{H}_B \end{pmatrix} = \mathbf{G}_{\text{th,R,AB}} \begin{pmatrix} T_A \\ T_B \end{pmatrix} + \begin{pmatrix} \dot{H}_{q,A} \\ \dot{H}_{q,B} \end{pmatrix} \quad (10)$$

and could be both arrived for the L- and the Pi- model. The derived enthalpy source values  $\dot{H}_{qR}$  given in Table II, fulfill the complete energy balance from (6) as well as the ECs' mesh equations. For the simplified systems for L- and Pi-EC the current sources representing  $\dot{H}_{qR}$  are zero and so can be eliminated from Fig. 2(a) and (b). For the T-EC only the SOE in (9) fulfilling the simplified energy balance in (5) in could be derived.

### C. Heat Supply and Demand

Heat generating units and customer requirements shall also be presented in electrical analogies and embedded as components in the ENM to provide a complete grid model. Since the return flow is not explicitly simulated here, the formulation of the generators and consumers as one-terminal components, i.e. A-components, is sufficient.

#### 1) Heat Supply Units:

Heat sources in the HN shall be regarded as a supply point with a given controlled pressure  $p_{q^*}$  and temperature  $T_{q^*}$ . It is named a  $p^*$ -component for the hydraulic system. For the thermal system it is named a  $T^*$ -component with the modified temperature  $T_{q^*,\text{mod}} = T_{q^*} - T_{\text{amb}}$  according to the definitions in (8). The components are displayed in Fig. 3(a) and (b) and equal ideal voltage sources. The components' terminal mass flow rates  $\dot{m}_p$  and enthalpy flows  $\dot{H}_p$  are a result of the calculation method presented here.

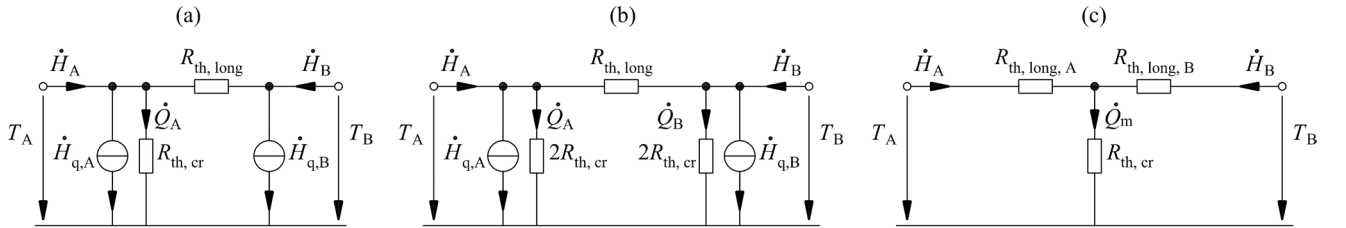


Fig. 2. Electric circuits for the steady-state modeling of a heating pipeline (a) Ladder-model (b) Pi-model (c) T-model.

TABLE II. ELECTRIC CIRCUIT PARAMETERS FOR THE THREE DIFFERENT HEATING PIPELINE MODELS, LADDER-, PI- AND T-MODEL.

	Ladder	Pi	T
$\dot{H}_{qR}$	$\begin{pmatrix} \frac{1}{R_{\text{th,long}}} \Delta e \\ -\frac{1}{R_{\text{th,long}}} \Delta e -  \dot{m}  c_p \Delta e \end{pmatrix}^T$	$\begin{pmatrix}  \dot{m}  c_p \Delta e (\frac{ \dot{m}  c_p}{G_{\text{th,cr}}} - \frac{1}{2}) \\  \dot{m}  c_p \Delta e (\frac{1}{2} - \frac{ \dot{m}  c_p}{G_{\text{th,cr}}}) -  \dot{m}  c_p \Delta e \end{pmatrix}$	/
$R_{\text{th,long}}$	$\frac{G_{\text{th,cr}}}{( \dot{m}  c_p)^2 - G_{\text{th,cr}}  \dot{m}  c_p}$	$\frac{G_{\text{th,cr}}}{( \dot{m}  c_p)^2 - \frac{G_{\text{th,cr}}^2}{4}}$	$R_{\text{th,A,T}} = \frac{1}{2 \dot{m}  c_p} (1 - \frac{ \dot{m}  c_p}{G_{\text{th,cr}}} - \frac{G_{\text{th,cr}}}{2})$ $R_{\text{th,B,T}} = \frac{1}{2 \dot{m}  c_p} (\frac{ \dot{m}  c_p}{G_{\text{th,cr}}} + \frac{G_{\text{th,cr}}}{2} - 1)$
$\mathbf{G}_{\text{th,R}}$	$\begin{pmatrix} G_{\text{th,cr}} + \frac{( \dot{m}  c_p)^2 - G_{\text{th,cr}}  \dot{m}  c_p}{G_{\text{th,cr}}} & -\frac{( \dot{m}  c_p)^2 - G_{\text{th,cr}}  \dot{m}  c_p}{G_{\text{th,cr}}} \\ -\frac{( \dot{m}  c_p)^2 - G_{\text{th,cr}}  \dot{m}  c_p}{G_{\text{th,cr}}} & \frac{( \dot{m}  c_p)^2 - G_{\text{th,cr}}  \dot{m}  c_p}{G_{\text{th,cr}}} \end{pmatrix}$	$\begin{pmatrix} \frac{G_{\text{th,cr}} + \frac{( \dot{m}  c_p)^2 - G_{\text{th,cr}}^2}{4}}{2} & -\frac{( \dot{m}  c_p)^2 - G_{\text{th,cr}}^2}{4 G_{\text{th,cr}}} \\ -\frac{( \dot{m}  c_p)^2 - G_{\text{th,cr}}^2}{4 G_{\text{th,cr}}} & \frac{G_{\text{th,cr}} + \frac{( \dot{m}  c_p)^2 - G_{\text{th,cr}}^2}{4}}{2} \end{pmatrix}$	$\begin{pmatrix} R_{\text{th,A,T}} + \frac{1}{G_{\text{th,cr}}} & \frac{1}{G_{\text{th,cr}}} \\ \frac{1}{G_{\text{th,cr}}} & R_{\text{th,B,T}} + \frac{1}{G_{\text{th,cr}}} \end{pmatrix}^{-1}$

## 2) Heat Demand Units:

Only directly connected heat consumer units shall be considered, so the required heat is taken directly as a mass-bound enthalpy flow  $\dot{H}$  from the supply system. The corresponding EC for the hydraulic as well as the thermal system are pictured in Fig. 3(c) and (d). If the consumers' mass flow rates  $\dot{m}_{A,d}$  are known, one hydraulic with a subsequent thermal calculation is sufficient. But for given consumers' heat demands  $\dot{Q}_{d*}$ , which are determined e.g. by forecast methods as presented in [16], the initial guess for the mass flow  $\dot{m}_{A,d}^0$  flowing into a consumer unit can be determined by

$$\dot{m}_{A,d}^0 = \frac{\dot{Q}_{d*}}{c_p(T_{q*} - T_{ret})} \quad (11)$$

which only exactly corresponds to the HN's setpoint temperature  $T_{q*}$  and is determined before the actual prevailing temperature at the connection point is known. With that mass flow rate, the consumer is set as a current source working as a sink with  $\dot{m}_{A,d} = \dot{m}_{qR}$  in the hydraulic system (see Fig. 3(c)). In the ENM, it is defined as an R-A-component with a conductance  $G_{h,R} = 0$ , representing that the mass flow is independent of the prevailing pressure and thus strictly speaking has no resistive behavior [14]. The value for  $\dot{m}_{A,d}$  has to be stepwisely adapted via an alternating algorithm between the hydraulic and the thermal consideration until  $\dot{Q}_{d*}$  is met (see Subsection III.C). In the thermal system, the consumers are represented using a thermal conductance  $G_{th,R}$  that establishes a correlation between potential  $T_A$  and flow quantity  $\dot{H}_A$  at its terminal, which is pictured in Fig. 3(d). This corresponds to the shape of an R-A component. The component's SOE can be written as:

$$\dot{H}_A = |\dot{m}_d| c_p T_A \quad (12)$$

corresponding to the definition of enthalpy flow rate as a mass-bound heat flow with  $G_{th,R,A} = |\dot{m}_d| c_p$  as the thermal conductance. To check, if the desired heat demand  $\dot{Q}_{d*}$  is met for each consumer  $i$ , the transformation from the modified temperature level to the real system is done with:

$$\dot{Q}_{d,i} = \dot{H}_{R,i} + \dot{m}_{R,i} c_p T_{amb} - \dot{m}_{R,i} c_p T_{ret} \quad (13)$$

## III. SYSTEM OF EQUATIONS IN THE EXTENDED NODE METHOD

Since the EC of the main HN components have been derived, now it is shown how they work in a grid system and how the node classification as well as the specific SOE are set up to a complete EEN in the context of the ENM.

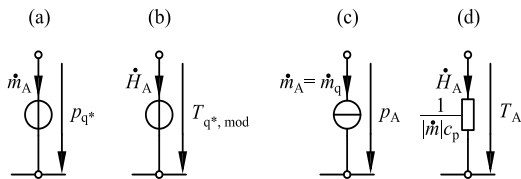


Fig. 3. Electric equivalents for Heat demand and Sources (a) Hydraulic Source (b) Thermal Source (c) Hydraulic demand (d) Thermal demand.

## A. Hydraulic System of Equations

Regarding steady hydraulic states, as derived in [14] for gas networks, a HN only consists of R- and p\*-components. The nodes are defined in such a way that only R-components are connected to R-nodes, while a node with a p\*-component is defined as a p\*-node. That leads to the following node equation system:

$$\begin{array}{l} \text{R-nodes} \\ \text{p*-nodes} \end{array} \begin{array}{l} \text{R-comp.} \\ \text{p*-comp.} \end{array} \begin{pmatrix} \mathbf{K}_{h,RR} & \mathbf{0} \\ \mathbf{K}_{h,p^*R} & \mathbf{K}_{h,p^*p^*} \end{pmatrix} \begin{pmatrix} \dot{\mathbf{m}}_R \\ \dot{\mathbf{m}}_{p^*} \end{pmatrix} = \mathbf{0}, \quad (14)$$

The hydraulic clamping matrices are given as  $\mathbf{K}_{h,RR}$  for R-components at R-nodes,  $\mathbf{K}_{h,p^*R}$  for R-nodes at p\*-nodes and  $\mathbf{K}_{h,p^*p^*}$  for p\*-components at p\*-nodes. They only consist of the values 0 (not connected) and 1 (connected). The vectors  $\dot{\mathbf{m}}_R$  and  $\dot{\mathbf{m}}_{p^*}$  contain of the mass flow rates of R- resp. p\*-components. A stable mass flow distribution for the R-components can be found with:

$$\dot{\mathbf{m}}_R = \mathbf{G}_{h,R} \mathbf{K}_{h,RR}^{-1} \mathbf{G}_{h,RR}^{-1} \mathbf{K}_{h,RR} \dot{\mathbf{m}}_{qR} + \dot{\mathbf{m}}_{qR} \quad (15)$$

with  $\mathbf{G}_{h,RR} = -\mathbf{K}_{h,RR} \mathbf{G}_{h,R} \mathbf{K}_{h,RR}^{-1}$  [4] and  $\dot{\mathbf{m}}_{qR}$  as the source mass flow rate vector including the source values from the heat consumers as R-A components (11) and the HPs as R-AB components (see (4)). The mass flow rates in  $\dot{\mathbf{m}}_{p^*}$  can be calculated by rearranging (14). Since the flow velocity  $v$  and the friction coefficients  $\lambda$  are unknown at the beginning, the conductance matrices  $\mathbf{G}_{h,R}^0$  resp.  $\mathbf{G}_{h,RR}^0$  are defined first, based only on geometric values [14] and are adapted during the process on basis of  $v$  and the Haaland Equation for  $\lambda$  with knowledge of the internal roughness  $k$ . The pressures at R-nodes can be determined by

$$\mathbf{p}_{RN} = \mathbf{G}_{h,RR}^{-1} (\mathbf{K}_{h,RR} \dot{\mathbf{m}}_{qR} - \mathbf{G}_{h,Rp^*} \mathbf{p}_{p^*N}) \quad (16)$$

with  $\mathbf{G}_{h,Rp^*} = -\mathbf{K}_{h,RR} \mathbf{G}_{h,R} \mathbf{K}_{h,p^*R}^{-1}$ .

## B. Thermal System of Equations

A steady thermal system transferred to its EEN only consists of R-components (HP and demand units) and T\*-components. The node classification is made according to the following scheme: If a T\*-component is connected to a node, it is classified as T\*-node, otherwise, if only R-components occur at a node, it is defined as an R-node. The node equations are then fulfilled with

$$\begin{array}{l} \text{R-nodes} \\ \text{T*-nodes} \end{array} \begin{array}{l} \text{R-comp.} \\ \text{T*-comp.} \end{array} \begin{pmatrix} \mathbf{K}_{th,RR} & \mathbf{0} \\ \mathbf{K}_{th,T^*R} & \mathbf{K}_{th,T^*T^*} \end{pmatrix} \begin{pmatrix} \dot{\mathbf{H}}_R \\ \dot{\mathbf{H}}_{T^*} \end{pmatrix} = \mathbf{0} \quad (17)$$

with the thermal clamping matrices  $\mathbf{K}_{th,RR}$  representing R-components at R-nodes,  $\mathbf{K}_{th,T^*R}$  for R-components at T\*-nodes and  $\mathbf{K}_{th,T^*T^*}$  for T\*-components at T\*-nodes. The thermal  $\mathbf{K}$ -matrices equal the hydraulic ones in (14), if the segmentation and node numbering are the same. The vector  $\dot{\mathbf{H}}_R$  includes the terminal enthalpy flows of the demand units as R-A-components and HP segments as R-AB components. The vector  $\dot{\mathbf{H}}_{T^*}$  represents the enthalpy flows from T\*-

controlled sources. The thermal conductance matrix  $\mathbf{G}_{th,R}$  has to be set up out of the single conductance matrices [4] of the thermal R-A components and R-AB-components as

$$\mathbf{G}_{th,R} = \begin{pmatrix} \mathbf{G}_{th,R,A} & \mathbf{0} \\ \mathbf{0} & \mathbf{G}_{th,R,AB} \end{pmatrix}. \quad (18)$$

With the help of the formulated node conductance matrices  $\mathbf{G}_{th,RR} = -\mathbf{K}_{th,RR} \mathbf{G}_{th,R} \mathbf{K}_{th,RR}^T$  and  $\mathbf{G}_{th,RT^*} = -\mathbf{K}_{th,RR} \mathbf{G}_{th,R} \mathbf{K}_{th,T^*R}^T$  in analogy to [4] the node  $\mathbf{T}_{RN}$  at R-nodes can be determined with

$$\mathbf{T}_{RN} = -\mathbf{G}_{RR,th}^{-1} (-\mathbf{K}_{th,RR} \dot{\mathbf{H}}_{qR} + \mathbf{G}_{RT^*} \mathbf{T}_{q^*,mod}). \quad (19)$$

$\dot{\mathbf{H}}_{qR} = (\mathbf{0}, \dot{\mathbf{H}}_{qR,AB})^T$  is the enthalpy source vector including the zero vector with the length of thermal R-A components and  $\dot{\mathbf{H}}_{qR,AB}$  with the enthalpy source values for the complete system as given in Table II. For the simplified system, it holds  $\dot{\mathbf{H}}_{qR} = \mathbf{0}$  since no source enthalpies occur. The components' terminal potentials can be derived from the network theory equation as:

$$\begin{pmatrix} \mathbf{T}_R \\ \mathbf{T}_{T^*} \end{pmatrix} = \begin{pmatrix} \mathbf{K}_{RR}^T & \mathbf{K}_{T^*R}^T \\ \mathbf{0} & \mathbf{K}_{T^*T^*}^T \end{pmatrix} \begin{pmatrix} \mathbf{T}_{RN} \\ \mathbf{T}_{T^*N} \end{pmatrix} \quad (20)$$

The terminal enthalpy flows  $\dot{\mathbf{H}}_R$  of the R-components can be calculated by:

$$\dot{\mathbf{H}}_R = \mathbf{G}_{th,R} \mathbf{T}_R + \dot{\mathbf{H}}_{qR} \quad (21)$$

and the enthalpy flows  $\dot{\mathbf{H}}_{T^*}$  of the T\*-components can be determined by rearranging (17).

### C. Hydraulic-Thermal Iteration Algorithm

An overall network condition can be determined with the help of an iteration algorithm between the hydraulic and the thermal system. The corresponding flowchart is pictured in Fig. 4. The complete algorithm runs as follows: First, based on a given heat demand  $\dot{Q}_{d^*}$  at the individual consumers, the associated mass flows  $\dot{m}_{A,d}^0$  of the consumers are determined with (11) by assuming the setpoint network temperature  $T_{q^*}$  at the consumer nodes. These are introduced as source mass flow rates  $\dot{m}_{qR}$  into the consumer components in the hydraulic system and go into the vector  $\dot{\mathbf{m}}_{qR}$ . The distribution of the mass flow rates over the HP as R-AB components is then determined with (15). Since the flow velocities are initially unknown, only the pipelines' geometric characteristics are taken to set up the initial hydraulic conductance matrices  $\mathbf{G}_{h,R}^0$  and  $\mathbf{G}_{h,RR}^0$ . This corresponds to a flow velocity of 1 m/s. In further steps, the conductances and hence the matrices are adjusted by the fact that the flow velocity is now known by the knowledge of the mass flow rate distributions  $\dot{\mathbf{m}}_R$ . The pressure distribution at the R-nodes  $\mathbf{p}_{RN}$  can then be determined with (16). The hydraulic iteration loop is terminated as soon as  $\dot{\mathbf{m}}_R$  and  $\mathbf{p}_{RN}$  no longer change significantly from one iteration step to the next. However, since the demand mass flow rates  $\dot{m}_{A,d}^0$  have been determined before the actual prevailing temperatures at the consumer nodes were known, the thermal calculation now takes place. The mass flow rates through the HP are included

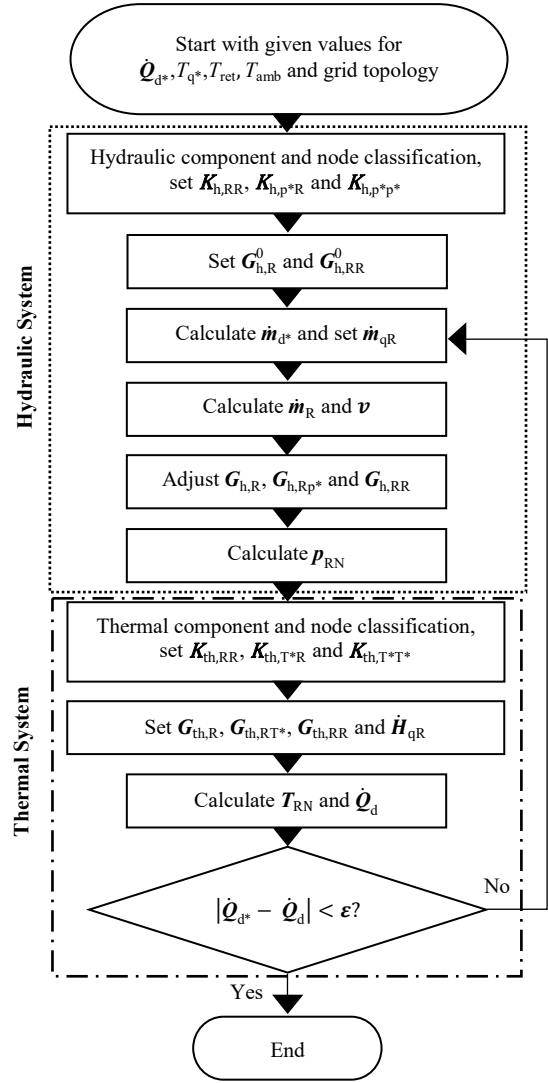


Fig. 4. Iteration algorithm of combined hydraulic and thermal calculation methodology.

in the parameters of the thermal EC. Thus the thermal conductance matrices  $\mathbf{G}_{th,R}$  and  $\mathbf{G}_{th,RR}$  can be built up and the temperature distribution is calculated according to (19). The amount of heat  $\dot{Q}_{d,i}$  now supplied to each consumer is given by (13), but after a first iteration step it does not yet correspond to the desired amount of heat  $\dot{Q}_{d^*,i}$ , since the associated mass flow rate was determined for the setpoint temperature  $T_{q^*}$ . In order to now meet the heat requirements, (11) is used with the prevailing node temperature  $T_{RN,j}$  instead. This allows an adjusted mass flow rate  $\dot{m}_{A,d,i}$  to be calculated. There follows again a hydraulic with following thermal calculations, until the deviations fulfill the termination criterion  $|\dot{Q}_{d^*,i} - \dot{Q}_{d,i}| < \epsilon$ .

## IV. STUDY CASES AND RESULTS

The three developed and presented EC, L-, Pi- and T-model, for HP shall be tested in two different HN configurations, one single line model and a further expanded grid. The study cases are compared with corresponding Simulink/Simscape simulations using the Thermal liquid (TL) library for the HN model. The water properties are set to  $\rho = \text{const.} = 1000 \text{ kg/m}^3$  and  $c_p = \text{const.} = 4200 \text{ J/(kgK)}$ . The ambient

temperature is  $T_{\text{amb}}=\text{const.}=285.15\text{ K}$  and the return temperature  $T_{\text{ret}}$  is set to  $323.15\text{ K}$ .

### A. Sample Single Line Heating Network

The single line model as pictured in Fig. 5 consists of one generation unit with  $T_{q^*}=373.15\text{ K}$  and  $p_{q^*}=16\text{ bar}$  at node 1 and one consumer unit with a fixed mass flow rate  $\dot{m}_{q^*}=2.1\text{ kg/s}$  at node 2 connected via a single HP with  $D_i=1.3\text{ m}$ ,  $D_o=1.3325\text{ m}$ ,  $D_{\text{ins}}=1.664\text{ m}$ ,  $l=1000\text{ m}$  and  $k=0.2\text{ mm}$ . The different EC and their results shall be compared in terms of different segment number. Fig. 6 displays the calculated temperature profile along the HP in  $x$ -direction for the L-model in Fig. 6(a), the Pi-model in 6(b) and the T-model in 6(c). The segment number was set to  $n_{\text{seg}}=1, 4, 16$  and  $64$ . The results were calculated with the simplified energy balance (5) ('s') for the T-model and for both, the simplified and complete energy balance (6) ('c') for the L- and Pi-model. Since Simulink cannot divide a pipeline of the TL-library into several segments for an incompressible calculation, only the controlled temperature at node 1 and the temperature at node 2 are shown. All three derived models have a slightly lower temperature at node 2 than the Simulink model. This is attributed to the fact that internally in the HP model of Simulink also a heat conduction from the center of the fluid to the wall is considered, while this is neglected in the model presented here. The convection term between fluid

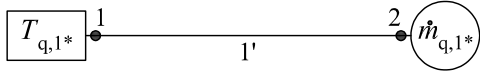


Fig. 5. Topology of single line heating network.

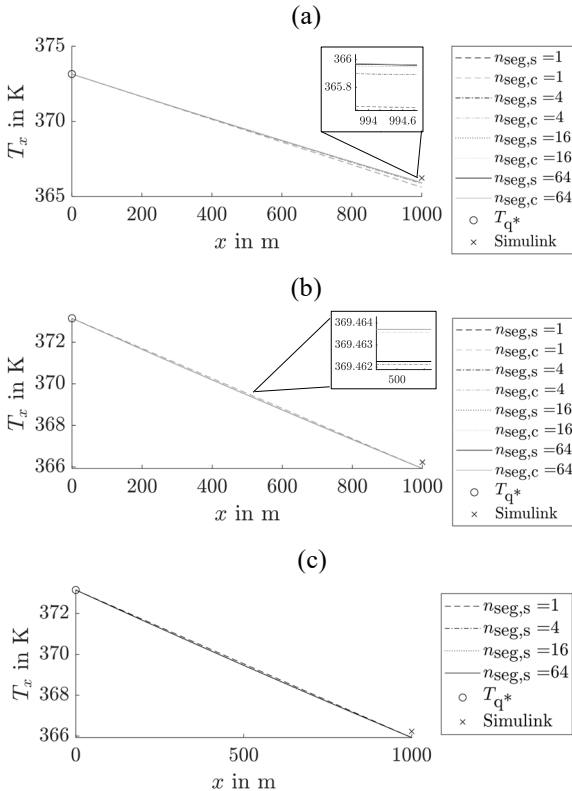


Fig. 6. Temperature curve along the heating pipeline in the single line heating network for different numbers of segments with comparison to Simulink (a) Ladder-model (b) Pi-model (c) T-model.

and pipeline wall occurs first in the thermal resistance  $R_{\text{th}}$  (see [9]). Fig. 6(a) also shows that the L-model with only one segment produces the coldest final temperature. This was to be expected, since the model assumes the controlled temperature  $T_{q^*}$  as the temperature for heat dissipation  $\dot{Q}_{\text{amb}}$  over the entire HP shell surface. If the number of segments in the L-model is increased, the temperature at node 2 also increases accordingly as can be seen in the zoom of Fig. 6(a). In principle, there is only a marginal difference in the other two models, T and Pi. Here, the number of segments rather determines the calculated temperature in the middle of the pipeline. In the zoom of Fig. 6, the difference between the energy balances is visible, but only to thousandths of a K. This is due to the very low pressure losses because of the low flow velocity here. For other conditions with higher pressure losses, it must be decided individually whether the term can still be neglected. In addition, it can be seen in the zoom of Fig. 6(b) that the result hardly changes from a segment number of  $n_{\text{seg}}=4$  to  $64$ . This is advantageous because for  $n_{\text{seg}}=4$ , the SOE and thus the computational effort is considerably much smaller.

### B. Sample 18-node Heating Network

As an example of a distinct HN topology, the configuration shown in Fig. 7, inspired by [15] with one feeder unit  $T_{q^*}=373.15\text{ K}$  and  $p_{q^*}=16\text{ bar}$  at node 1, 17 pipelines (1' to 7'), 10 heat customers  $\dot{H}_{q,1}$  to  $\dot{H}_{q,10}$  and a total of 18 nodes is used. The HP parameters are listed in Table III. In order to simplify the comparison with Simulink, fixed mass flows for the heat consumers have been defined as  $\dot{m}_{q,1}=2.5\text{ kg/s}$ ,  $\dot{m}_{q,2}=3.0\text{ kg/s}$ ,  $\dot{m}_{q,3}=2.1\text{ kg/s}$ ,  $\dot{m}_{q,4}=4.0\text{ kg/s}$ ,  $\dot{m}_{q,5}=1.2\text{ kg/s}$ ,  $\dot{m}_{q,6}=2.3\text{ kg/s}$ ,  $\dot{m}_{q,7}=2.3\text{ kg/s}$ ,  $\dot{m}_{q,8}=2.8\text{ kg/s}$ ,  $\dot{m}_{q,9}=3.1\text{ kg/s}$  and  $\dot{m}_{q,10}=4.1\text{ kg/s}$ . Since again no significant differences for the two versions of the energy balance in (5) and (6) were visible, only the results for the simplified energy balance are presented below. They are pictured in Fig. 8 for a chosen segment number of  $n_{\text{seg}}=4$  per HP 1'-17'. In Fig. 8(a), the absolute node temperatures  $T_N$  at the nodes 1-18 are displayed. These show very good agreement with the results from Simulink. For better comparability, relative quantities are chosen. Fig. 8(b) plots the relative node pressures  $p_{N,\text{rel}}=p_{\text{ENM}}/p_{\text{Sim}}$ . The hydraulic model is independent of the thermal ECs, therefore only one result

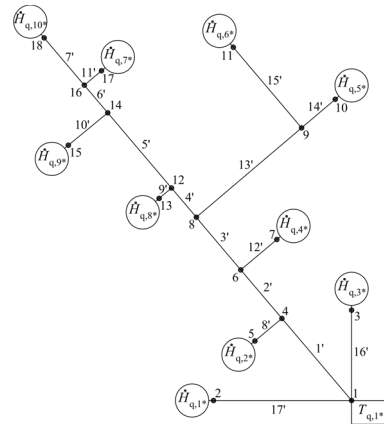


Fig. 7. 18-node sample heating network topology, inspired from [11].

TABLE III. HEATING PIPELINES' GEOMETRIC PARAMETERS FOR 18-NODE HEATING NETWORK.

No.	A	B	$D_i$ in m	$D_o$ in m	$D_{ins}$ in m	$l$ in m	$k$ in mm
1'	1	4	3.5	3.5875	4.4800	200	0.2
2'	4	6	3.5	3.5875	4.4800	120	0.2
3'	6	8	3.5	3.5875	4.4800	80	0.2
4'	8	12	3.5	3.5875	4.4800	35	0.2
5'	12	14	3.5	3.5875	4.4800	150	0.2
6'	14	16	3.0	3.0750	3.8400	20	0.2
7'	16	18	3.0	3.0750	3.8400	210	0.2
8'	4	5	2.5	2.5625	3.2000	50	0.2
9'	12	13	2.5	2.5625	3.2000	55	0.2
10'	14	15	3.0	3.0750	3.8400	210	0.2
11'	16	17	2.2	2.2550	2.816	50	0.2
12'	6	7	3.0	3.0750	3.8400	50	0.2
13'	8	9	3.0	3.0750	3.8400	180	0.2
14'	9	10	1.6	1.6400	2.0480	10	0.2
15'	9	11	1.5	1.5375	1.9200	300	0.2
16'	1	3	1.3	1.3325	1.6640	200	0.2
17'	1	2	1.6	1.6400	2.0480	370	0.2

graph is shown. The deviations from the generated result to Simulink are negligible. In Fig. 8(c), the relative nodal temperatures  $T_{N,rel} = T_{ENM}/T_{Sim}$  and in 8(d), the relative heat dissipated  $\dot{Q}_{HP,rel} = \dot{Q}_{ENM}/\dot{Q}_{Sim}$  via the HP are pictured. It gets obvious that the values of the heat flow rates  $\dot{Q}_{ENM}$  to the environment computed with the ENM are higher than in the Simulink simulation. Accordingly, that leads to lower temperatures (see Fig. 8(c)), which was also the case for the single-line model. The largest relative deviation occurs here at the shortest HP 14' and amounts to about 2.6 percent. For the line lengths present in the sample HN, the difference in pressures and temperatures is hardly noticeable.

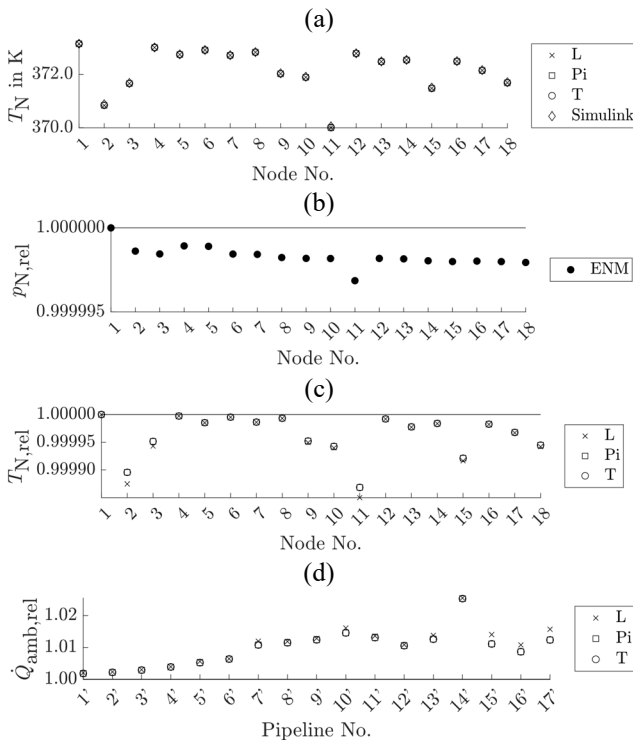


Fig. 8. Results for 18-node heating network with comparison to Simulink. (a) Absolute node temperatures (b) Relative node pressures (c) Relative node temperatures (d) Relative Pipelines' released heat flow to the environment.

## V. CONCLUSION AND OUTLOOK

The outcomes of the here presented paper can be concluded as follows:

- Three different EC-models, a Ladder-, a Pi- and a T-model for the thermal description of HP resp. segments have been derived
- These EC are obtained without additional current sources for a simplified energy balance. For the complete energy balance, the current sources have been specified for the L- and the Pi-model.
- The developed EC have been declared as components of the ENM and been embedded into the method's SOE to enable the finding of stable steady operating points also for extended networks
- Generated results have been compared with Simulink/Simscape and show substantial consensus

Following the algorithm developed here for determining steady states for HN, further development stages of the model, e.g. for hydraulically and thermally unsteady operation, must be regarded and set into the context of the ENM. In the long term, the connection with electric and gas networks is planned via appropriate coupling technologies like e.g. fuel cells as in [17] in the sense of the ENM.

## VI. ACKNOWLEDGMENT

This work has been created during the project "integrated network planning: Development of a network development planning methodology for the joint planning of the three energy sources electricity, gas and heat" funded by Federal Ministry for Economic Affairs and Climate Action with the grant number 03EWR007H2.

## REFERENCES

- [1] H. Lill, A. Allik, M. Hovi, K. Loite and A. Annuk, "Integrated Smart Heating System in Historic Buildings," in *7th IEEE International Conference on Smart Grid (icSmartGrid)*, Newcastle, Australia, December 9-11, 2019.
- [2] F. Huang, J. Lu, J. Zheng, F. Huang and J. Baleynaud, "Feasibility of Heat Recovery for District Heating Based on Cloud Computing Industrial Park," in *4th International Conference on Renewable Energy Research and Applications (ICRERA)*, Palermo, Italy, November 22-25, 2015.
- [3] L. Hofmann, Efficient computation of transients in extended electric power systems, German: Effiziente Berechnung von Ausgleichsvorgängen in ausgedehnten Elektroenergiesystemen (Berichte aus der Elektrotechnik), 1 ed., Shaker, 2003.
- [4] B. R. Oswald, Calculation of three-phase networks; calculation of stationary and non-stationary processes with symmetrical components and space phasors, German: Berechnung von Drehstromnetzen, 4 ed., Wiesbaden: Springer Vieweg Wiesbaden, 2021.
- [5] S. Hakimizad, S. Razzaghi Asl and M. Mehdi Ghiai, "A Review on the Design Approaches Using Renewable Energies in Urban Parks," *International Journal of Renewable Energy Research*, vol. 5, pp. 686-693, 2015.
- [6] V. Amir, S. Jadid and M. Ehsan, "Optimal Planning of a Multi-Carrier Microgrid (MCMG) Considering Demand-Side Management," *International Journal of Renewable Energy Research*, vol. 8, pp. 238-249, March 2018.
- [7] R. Song, Y. Xia, Y. Chen, S. Du, K. Strunz, Y. Song and W. Fang, "Efficient modelling of natural gas pipeline on electromagnetic transient simulation programs," *IET Renewable Power Generation*, pp. 186-198, 26 March 2022.
- [8] M. Taherinejad, S. M. Hosseinalipour and R. Madoliat, "Steady flow analysis and modeling of the gas distribution network using the electrical analogy," *International Journal of Engineering*,

*Transactions B: Applications*, Vols. 27, No. 8, pp. 1269-1276, August 2014.

- [9] T. Lan and K. Strunz, "Modeling of the Enthalpy Flow Using Electric Circuit Equivalents: Theory and Application to Transients of Multi-Carrier Energy Systems," *IEEE Transactions on Energy Conversion*, vol. No. 4, pp. 1720-1730, December 2019.
- [10] J. Chen, F. Li, H. Li, B. Sun, C. Zhang and S. Liu, "Novel dynamic equivalent circuit model of integrated energy systems," *Energy*, vol. Part A, 2023.
- [11] Z. Pan, Q. Guo and H. Sun, "Interactions of district electricity and heating systems considering time-scale characteristics based on quasi-steady multi-energy flow," *Applied Energy*, pp. 230-243, April 2016.
- [12] H. Liu, X. Liu and Q. Jin, "A new power flow model for combined heat and electricity analysis in an integrated energy system," *Applied Thermal Engineering*, vol. Part B, 2023.
- [13] L. Hao, F. Xu, Q. Chen, M. Wei, L. Chen and Y. Min, "A thermal-electrical analogy transient model of district heating pipelines for integrated analysis of thermal and power systems," *Applied Thermal Engineering*, pp. 213-221, July 2018.
- [14] D. Vorwerk and D. Schulz, "Steady-state and unsteady Gas Grid Calculation with the Extended Node Method based on Electrical Analogies," *Submitted to: Sustainable Energy, Grids and Networks [unpublished]*, 2023.
- [15] B. Glück, Heating water networks for residential and industrial areas, German: Heizwassernetze für Wohn- und Industriegebiete, 1. Auflage ed., VEB Verlag für Bauwesen Berlin, 1985.
- [16] J. A. Thomas, "Prediction of Heat Demand for Building Energy Managers: An IoT and Control Perspective," in *8th IEEE International Conference on Smart Grid (icSmartGrid)*, Paris, France, June 17-19, 2020.
- [17] B. Zafar, "Design of a Renewable hybrid photovoltaic-Electrolyze-PEM/Fuel Cell System using Hydrogen Gas," *International Journal of Smart Grid*, vol. 3, pp. 201-207, December 2019.